

Solar chimney: modelling and verification

D. Lanceta, J. Llorente

Renewable Energy Centre (CENER), Spain

ABSTRACT

In this article, the first part of a research project about the modelling of a solar chimney is presented. In this first part, the average ventilation flows measured in an experimental installation have been compared to the results obtained by CFD (Computational Fluid Dynamics) simulations. In order to do so, a solar chimney with a cross-section of 0.78 m x 0.156 m, height 3.6 m, has been constructed. The chimney consists of a glass surface oriented towards the south. The internal (absorber) surface is made of a copper plate, which has been painted black in order to increase the solar absorption. The chimney is connected to a room measuring 5 m x 2.5 m x 2.5 m, from where it extracts air.

The modelling of natural ventilation openings is usually done by specifying the discharge coefficient, which relates the air velocity of the ventilation flow with a pressure difference. In the case of modelling a solar chimney, the effect of buoyancy caused by the hot chimney surfaces should be taken into account as well as the discharge coefficient's dependence of the external wind.

The data acquisition system used in this first part of the project measures the ventilation flow, the absorber and glass temperatures and the pressure difference between the chimney inlet and outlet.

The comparison of the results obtained by measurements with those obtained by CFD simulations show that computational tools are accurate enough to predict the behaviour of natural buoyancy in this kind of installations.



Figure 1: Solar chimney test rig.

In a later stage of the project the relationship between the external wind field and the pressure difference will be investigated and a mathematical model to predict the absorber and glass temperatures will be developed.

1. INTRODUCTION

Besides improving the indoor air quality, natural ventilation in buildings can contribute to an important reduction of cooling loads.

Conventional ventilation chimneys are based on the stack effect, which occurs when the temperature inside the chimney is higher than the exterior temperature. The driving force depends on the difference in density between the external and internal air.

A solar chimney is a ventilation chimney of which one or more walls are replaced by a transparent surface. The transparent walls allow solar radiation to enter into the solar chimney, where it is being absorbed. A large part of the radiation absorbed by the interior walls, heat up the air inside the chimney, increasing the driving force of the chimney draught.

Some interesting articles related to the working of solar chimneys are the following: Afonso and Oliveira (1999) in which the working of a solar chimney is being compared to that of a conventional one, Ong (2002) in which a mathematical model is developed to model the working of a solar chimney, Khedari et al. (2001) in which the potential reduction in energy consumption is being showed when coupling a solar chimney with an air conditioning system. An analytical study of a solar chimney coupled to a wind tower is presented in Bansal et al. (1994)

2. THEORY

2.1 General theory

Envelope flow models of ventilation are mathematical models that describe the flows through the envelope of a building. The flow rate (unidirectional) through an opening is determined from knowledge of its still-air discharge coefficient, which is defined by:

$$C_z = \frac{q}{A} \sqrt{\frac{\rho}{2\Delta P}} = u \sqrt{\frac{\rho}{2\Delta P}} = f(\text{Re}) \quad (1)$$

C_z : Still air discharge coefficient (dimensionless)

q : Volume flow rate through opening (m^3/s)

A: Area of opening (m²)
 ρ: Density (kg/m³)
 u: Flow velocity (m/s)
 ΔP: Static pressure difference (hydrostatic pressure difference not included) (Pa)
 Under still-air conditions, C_z is fixed purely by the shape of the opening and the Reynolds number, Re, defined by:

$$Re = \frac{\rho u L}{\mu} \quad (2)$$

Re: Reynolds number (dimensionless)
 L: Characteristic dimension (m)
 μ: Viscosity (m²/s)

In stack ventilation ducts, the ventilation flow is not under still air conditions at the outlet, because of the influence of wind. To determine the discharge coefficient of the chimney without the influence of the external wind flow, the outlet pressure tap is located in the inner part of the chimney, 20 cm below the outlet. (See Chiu and Etheridge 2006).

When using the steady state discharge coefficient (equation (1)), the inertia of the mass of the air which is accelerated under unsteady conditions, is not taken into account. The mathematical model proposed in Etheridge (1999), known as Quasi-steady/temporal inertia assumption, has been used to adjust the instantaneous values (equation (3)).

$$q^2 \{t\} S_q + 2C_z A l_e \frac{dq \{t\}}{dt} = 2C_z^2 A^2 \frac{\Delta P \{t\}}{\rho} \quad (3)$$

l_e: Effective length of the opening (m)
 S_q: Sign of q

The term l_e denotes the so-called effective length of the opening and takes into account the inertia of the air column. It is usually determined empirically.

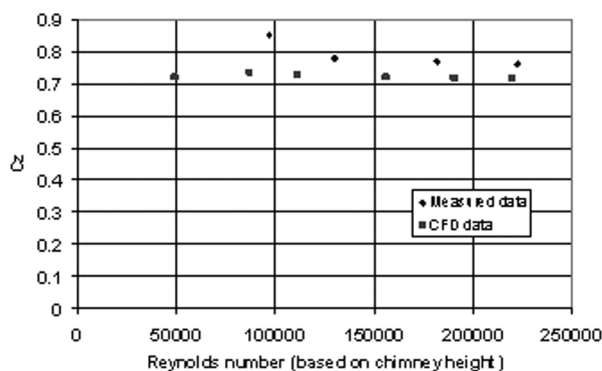


Figure 2: Discharge coefficient.

In Figure 2, the discharge coefficient measured in the CENER solar chimney (by night, no buoyancy effect) is compared with CFD simulations. CFD model and experimental rig characteristics will be presented below.

In Figure 2 it can be seen that within the calculated Reynolds range, the CFD discharge coefficient is basically constant. The experimental results show a similar tendency. The effective length of the chimney l_e is about 2.5 m.

2.2 Buoyancy modelling

2.2.1 Buoyancy in normal ventilation chimneys

The buoyancy pressure resulting from the difference between the internal and the external temperatures can be calculated with equation (4). The ventilation flow can be determined from this pressure difference and the discharge coefficient.

$$\Delta P = (\Delta \rho) g H = \rho \beta (T_{air} - T_{amb}) g H \quad (4)$$

T_{air}: Air temperature inside the chimney (K)
 T_{amb}: Ambient air temperature (K)
 β: Volumetric thermal expansion coefficient (K⁻¹)
 H: Chimney height (m)

2.2.2 Buoyancy in solar chimneys

In a solar chimney, there is an additional contribution to the stack effect due to the increase in air temperature as it flows through the chimney.

In this project, in order to take this heating effect into account in the model, a correction is made in the discharge coefficient. A dimensionless number analysis shows that, in that case, this coefficient would depend not only on the Reynolds number but also on additional dimensionless numbers containing the temperature difference between the chimney wall/glass and the air temperature at the inlet (equations (5) & (6)).

$$C_z = f(Re, Gr_{abs}, Gr_{glass}) \quad (5)$$

$$Gr_x = \frac{\rho^2 g \beta (T_x - T_{air,inlet}) L^3}{\mu^2} \quad (6)$$

Gr: Grashof number (dimensionless)
 T_x: Temperature of absorber or glass (K)
 T_{air,inlet}: Air temperature at chimney inlet (K)
 β: Volumetric thermal expansion coefficient (K⁻¹)
 L: Characteristic dimension (m)

If the fluid of work is air, the results obtained in this paper can be extrapolated to similar geometries (height/width = 3.6/0.155 = 23), by means of these dimensionless numbers.

3. CFD STUDY

The experimental data has been compared with the results of a CFD model. The model has been supplied directly with the boundary conditions measured in the experimental installation: wall temperatures and pressure differences between the entrance and exit. In this

way, it is expected that the obtained differences between measurement and simulation will be minimal. Now the characteristics of the CFD model will be presented.

3.1 Computational model

- The problem has been approximated by assuming that it is two dimensional and stationary, basically to reduce calculation time and to be able to solve the flow near the walls more precisely.
- The number of cells has been 90744, which has been determined from grid dependency tests. The mesh size allows having a y^+ value lower than 1 in the wall zone.
- The used values for density, viscosity, specific heat and conductivity of air are those at 25°C and atmospheric pressure.
- The density is considered to be constant and the buoyancy is modelled using the approximation of Boussinesq.
- The applied turbulence model has been the k- ϵ Standard by Launder and Spalding (1974)
- The wall zone has been modelled with a two-layer model, which allows the solving of the part of the flow affected by viscosity by means of the Wolfstein equation (1969).
- The pressure-velocity coupling has been done by applying the SIMPLE model and the discretisation of the variables has been of the second order.

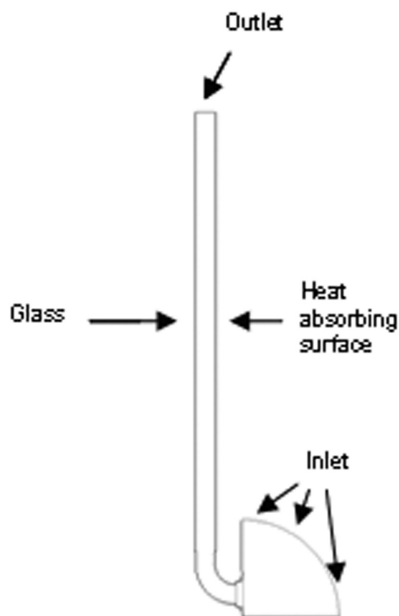


Figure 3: Boundary conditions.

3.2 Boundary conditions

- The applied boundary conditions have been the following:
- Inlet: The pressure and temperature conditions are constant and equal to those of the room. The air enters the solar chimney under still-air conditions.
 - Outlet: A constant pressure is assumed in the final part

of the chimney. The height where the boundary condition is applied coincides with the position of the pressure tap in the experimental installation, 20 cm below the exit of the chimney. In case of having a reversed flow, the air enters with the exterior temperature.

- *Heat absorbing surface & Glass*: The walls are modelled as smooth walls at a constant temperature.

3.3 Operating conditions

Buoyancy is modelled as a volumetric force proportional to the temperature difference with the ambient temperature. In the simulations is assumed that the inlet (room) temperature is always equal to the ambient temperature. However in reality the temperature in the room could be different from the ambient temperature, which will cause an additional buoyancy flow. To take this effect into account an additional pressure difference should be incorporated into the pressure term. In this way, the ΔT responsible for the buoyancy caused by solar radiation is temperature difference between the glass/wall temperature in the chimney and the air-inlet (equations (7) & (8)).

$$\Delta T_{glass} = T_{glass} - T_{air\,inlet} \quad (7)$$

$$\Delta T_{abs} = T_{abs} - T_{air\,inlet} \quad (8)$$

3.4 Cfd results

In this paragraph, the CFD results will be presented:

ΔP : Pressure difference due to wind and/or buoyancy caused by temperature difference between room and ambient.

ΔT_{abs} : Temperature difference between absorber plate and inlet air temperature.

ΔT_{glass} : Temperature difference between glass and inlet air temperature.

u : Mean velocity.

In the following graphs the relationship between pressure difference, absorber temperature difference and mean velocity is presented for three different values of glass temperature difference.

Example: when the wind causes a pressure difference of 0.3 Pa and there is no solar radiation, the mean velocity of the air flow in the unheated chimney will be 0.45 m/s. If then, the sun starts shining and the absorber temperature would increase 40° C above inlet temperature ($\Delta T_{abs}=40$) and the glass temperature would be 10° C above inlet temperature ($\Delta T_{glass}=10$), then the mean velocity will be about 0.7 m/s. (See Figure 5).

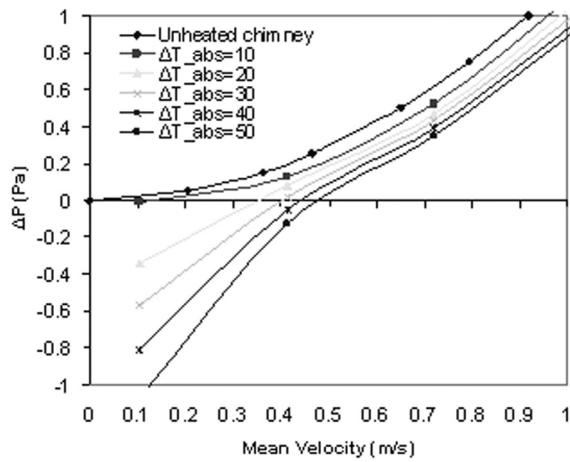


Figure 4: CFD results for $\Delta T_{\text{glass}} = 0$.

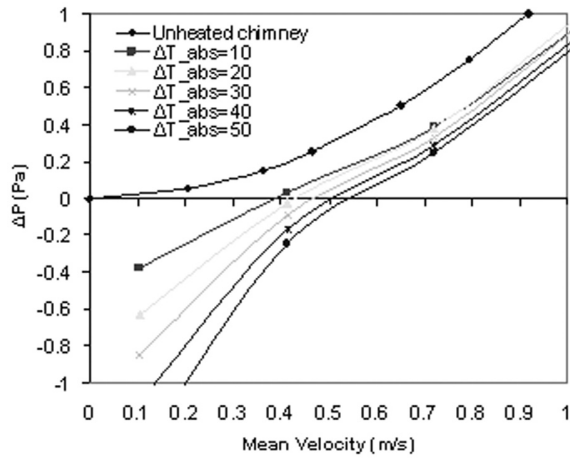


Figure 5: CFD results for $\Delta T_{\text{glass}} = 10$.

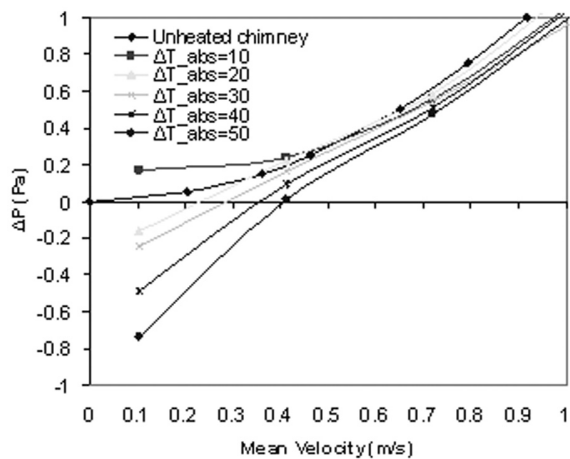


Figure 6: CFD results for $\Delta T_{\text{glass}} = -10$.

4. EXPERIMENTAL WORK

4.1 Test rig set up

The experimental installation consists of an aluminium

U-profile, insulated with 4 cm of mineral wool, on which a 1 mm thick black copper plate has been placed. In the external wall a highly transparent glass has been applied. The size of the horizontal cross-section of the solar chimney is 0.782 m (width) by 0.156 m (depth, the distance between glass and absorber). The height of the straight part of the chimney is 3.6 meters. At the bottom of the chimney a curved 90°-angle piece connects the chimney to the room, having the same cross section as the chimney itself throughout the entire curve. The size of the room (a container) is approximately 5 m x 2.5 m x 2.5 and has the possibility of sizing and moving several inlets and exits, depending on the type of experiment.

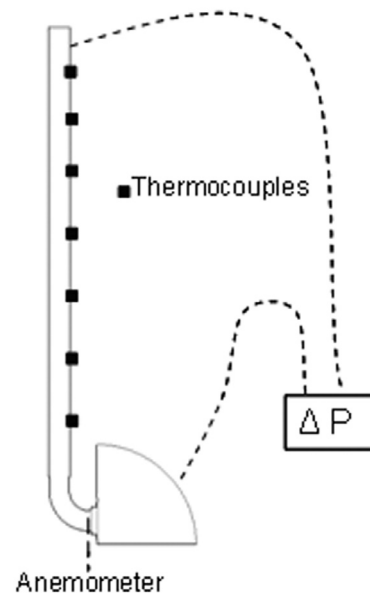


Figure 7: Instrumentation.

4.2 Instrumentation

Mounted on the backside, throughout the height of the copper absorber plate (3.6 m) there are 7 thermocouples (T-type). The pressure difference between the pressure tap near the chimney outlet and the pressure tap at the inlet, is measured with the micromanometer Furness FCO44, calibrated in the range of +40/-40 Pa.

The ventilation flow inside the chimney is measured with an anemometer situated in the curved 90°-angle piece at the bottom of the chimney. The anemometer, Schmidt SS 20.400 is able to detect the direction of the flow and is calibrated in the range of -1/+1 m/s.

The sample time for velocities and pressures has been 6 Hz, enough to register the majority of pressure fluctuations due to the external wind. The presented experimental data are averaged values based on instantaneous values. During the measurements has been strived towards having a temperature at the inlet of the chimney equal to the ambient temperature. Table 1 shows the

measured values and the values coming from the CFD simulations. As can be seen, the measured velocities are quite similar to those predicted by the CFD model.

Table 1: Results

| ΔP (Pa) | ΔT (°C) | | V (m/s) | |
|-----------------|-----------------|----------|---------|------|
| | Exp.&CFD | Absorber | Glass | Exp. |
| -0.25 | 37.9 | 8.9 | 0.29 | 0.34 |
| -0.11 | 42.8 | 9.3 | 0.39 | 0.44 |
| +0.14 | 39.9 | 8.6 | 0.55 | 0.61 |
| +0.35 | 42.0 | 8.5 | 0.69 | 0.76 |
| +1.13 | 37.8 | 5.8 | 0.97 | 1.11 |
| +0.1 | 12.4 | 1.9 | 0.40 | 0.37 |
| +0.29 | 12.3 | 0.3 | 0.54 | 0.56 |
| +0.13 | 26.3 | 3.1 | 0.44 | 0.49 |
| +0.24 | 20.4 | 2.6 | 0.53 | 0.54 |
| +0.34 | 13.7 | 2.1 | 0.60 | 0.62 |
| +0.70 | 18.8 | 1.9 | 0.87 | 0.84 |
| +1.00 | 35.4 | 2.9 | 1.02 | 1.04 |
| -0.15 | 35.4 | 4.3 | 0.39 | 0.37 |
| +0.09 | 42.8 | 5.1 | 0.57 | 0.54 |
| +0.27 | 45.2 | 5.9 | 0.70 | 0.67 |
| +0.63 | 45.8 | 6.5 | 0.88 | 0.86 |
| +1.04 | 42.0 | 5.5 | 1.04 | 1.07 |
| -0.15 | 19.8 | 2 | 0.29 | 0.24 |
| -0.04 | 19.1 | 2.5 | 0.36 | 0.32 |
| +0.17 | 18.5 | 2.7 | 0.56 | 0.48 |
| +0.49 | 22.8 | 4 | 0.74 | 0.73 |
| +0.97 | 18.7 | 2.6 | 0.96 | 0.96 |
| -0.27 | 37.4 | 5.9 | 0.31 | 0.34 |
| +0.00 | 36.9 | 4.6 | 0.45 | 0.47 |
| +0.24 | 37.6 | 5.4 | 0.59 | 0.66 |
| +0.51 | 37.9 | 5.8 | 0.79 | 0.82 |
| +0.88 | 36.6 | 5.6 | 0.94 | 1.00 |

5. CONCLUSIONS

The comparison of the results obtained by measurements with those obtained by CFD simulations (table 1) show that computational tools are accurate enough to predict the behaviour of natural buoyancy in solar chimney installations.

ACKNOWLEDGEMENTS

This research was funded by the Spanish Ministry of Education and Science. Their support is gratefully acknowledged.

REFERENCES

- Afonso, C. & Oliveira, A. (1999). Solar chimneys: simulation and experiment. *Energy and Buildings*, Vol. 32: 71-79.
- Bansal, N.K., Rajesh Mathur & Bhandari, M.S. (1994). A study of solar chimney assisted wind tower system for natural ventilation in buildings. *Building and Environment*, Vol. 29: 495-500.
- Chiu, Y-H. & Etheridge, D.W. (2006). External flow effects on the discharge coefficients of two types of ventilation opening. *Journal of Wind Engineering and Industrial Aerodynamics*, Vol. 95: 225-252.
- Etheridge, D.W. (1999). Unsteady flow effects due to fluctuating wind pressures in natural ventilation design-mean flow rates. *Building and Environment*, Vol. 35: 111-133.
- Khedari, J., Rachapradit, N. & Hirunlabh, J. (2001). Field study of performance of solar chimney with air-conditioned building. *Energy*, Vol. 28: 1099-1114.
- Launder, B.E. & Spalding, D.B. (1974). The numerical computation of turbulent flows. *Computer Methods in Applied Mechanics and Engineering*, Vol. 3: 269-289.
- Ong, K.S. (2002). A mathematical model of a solar chimney. *Renewable Energy*, Vol. 28: 1047-1060.
- Wolfstein, M. (1969). The velocity and temperature distribution of one-dimensional flow with turbulence augmentation and pressure gradient. *International Journal of Heat & Mass Transfer*, Vol. 12: 301-318.